TÜBİTAK

Turkish Journal of Physics

http://journals.tubitak.gov.tr/physics/

Research Article

Turk J Phys
(2017) 41: 359 – 366

doi:10.3906/fiz-1704-6

# Annealing and deposition time effects on the structural, optical, and electrical properties of indium sulfide thin films produced by chemical bath deposition method

**Emine GÜNERİ**[1,*], **Fatma GÖDE**[2]

[1]Department of Primary Education, Faculty of Education, Erciyes University, Kayseri, Turkey
[2]Department of Physics, Faculty of Arts and Sciences, Mehmet Akif Ersoy University, Burdur, Turkey

**Received:** 06.04.2017 • **Accepted/Published Online:** 12.06.2017 • **Final Version:** 05.09.2017

**Abstract:** Indium sulfide thin films were deposited onto indium-doped tin-oxide substrates with different deposition times (60 h, 63 h, 66 h, and 69 h) at room temperature by using a chemical bath deposition method to obtain new structures for solar cells. The film obtained at 60 h was annealed at 400 °C for 1 h in nitrogen media. The crystallographic structure of the films was observed via the X-ray diffraction pattern while the size and shape of the grains were characterized by scanning electron microscopy. Moreover, the optical transmission spectra of the films were obtained at room temperature in the wavelength range of 300–1100 nm. After the films were annealed, the optical transmission decreased from 52% to 26% at a wavelength of 550 nm. With increasing film thickness and grain size, the direct and indirect optical band gap of the InS films decreased from 2.31 eV to 2.19 eV and from 1.89 eV to 1.75 eV, respectively. The refractive index, extinction coefficient, and dielectric constant of the films were determined. The sheet resistivity of the films decreased from 33 Ω cm to 28 Ω cm with increasing grain size.

**Key words:** Indium sulfide, thin films, annealing, optical properties

## 1. Introduction

A great number of researchers are working to find materials that are energy-related and environmentally friendly for use in optoelectronics, the photovoltaic industries, and photoelectrochemical solar cell devices. Some of the III–VI semiconductor compounds have good optoelectronic properties, such as indium selenide ($In_2Se_3$), germanium selenide (GaSe), and indium sulfide (InS). InS, being a nontoxic material, has a stable chemical composition and physical characteristics at room temperature. This material seems to be promising for technological applications because of its high transmittance (70%–80%) in the visible range, high band gap energy (2–3.7 eV), and photoconductor behavior. It has three phases (?, ?s and ?), depending on the temperature and conditions of deposition [1–4].

InS thin films have been prepared by several dry and wet techniques, such as thermal evaporation [5], chemical vapor deposition [6], successive ionic layer adsorption and reaction [3], spray pyrolysis [7], and chemical bath deposition (CBD) [8]. Among them, CBD has been preferred by many researchers because it is an inexpensive, simple, and convenient method to obtain thin film.

In this work, we investigated the annealing and deposition time effects on the structural optical and

*Correspondence: emineg7@gmail.com

electrical properties of InS thin films produced by the CBD technique. To the best of our knowledge, there are few reports in the literature on the deposition of InS thin films deposited by using the CBD method.

## 2. Experimental details

Indium sulfide thin films were grown on indium-doped tin-oxide (ITO) (R = 9.5 $\Omega$/sq.) substrates (7.6 cm $\times$ 2.6 cm $\times$ 0.1 cm) by using the CBD technique. The reagents used for the preparation of indium sulfide thin films were as follows: 10 mL of 0.1 M indium chloride [$InCl_3$; Aldrich; $\geq$99.99% purity], 0.3 mL of 3.15 M triethanolamine [$HOCH_2CH_2)_3N$; Merck; 99% purity], 20 mL of 0.2 M acetic acid ($CH_3COOH$; Merck; 100% purity), and 20 mL of 0.4 M thioacetamide ($CH_3CSNH_2$; Merck; ACS Reag.). The total solution volume was completed to 50 mL by adding deionized water. The final pH of the solution was measured as 3.72. The films were prepared by immersing the substrates vertically into the aqueous solution. The films were obtained at room temperature (30 °C) from the acidic solution with different deposition times such as 60 h, 63 h, 66 h, and 69 h in order to obtain different film thicknesses such as 688 nm, 735 nm, 780 nm, and 860 nm, respectively. After the deposition, the thin films were rinsed in deionized water to remove loosely adhered particles on the film surface and then dried in air. The film deposited at 60 h with the thickness of 688 nm was annealed at 400 °C for 1 h in reduced media containing 90% $N_2$ and 10% $H_2$.

The X-ray powder diffraction (XRD) patterns were recorded using a Bruker AXS D8 diffractometer system with Cu K$\alpha$ (1.54 Å) radiation. The surface morphology and cross-sectional images of the films were studied using EVO40-LEO scanning electron microscopy (SEM). The optical transmittance spectra were measured on a PerkinElmer Lambda 4S UV-Vis spectrophotometer in the wavelength range of 300–1100 nm using a glass substrate as the reference. Electrical measurements were carried out using a computer-controlled Keithley 2400 current voltage (I–V) source measuring system.

## 3. Results and discussion

### 3.1. Structural properties of indium sulfide thin films

Figure 1 shows the XRD patterns of the as-grown and annealed thin films. The XRD patterns reveal that the thin films obtained at room temperature are poorly polycrystalline in the orthorhombic structure InS (PDF 19-0588). When the films are annealed at 400° C, they show a mixture of InS (PDF 19-0588) and $In_2S_3$ (PDF 25-0390). The crystal structure has poor polycrystallinity even though all peak intensities on the XRD spectra increase with annealing. This increase in peak intensity results from the change in the grain size after the annealing process. Figure 2 shows the SEM images of the ITO substrate, as-grown film, annealed film, and cross-section view of the indium sulfide thin film produced at 60 h with the thickness of 688 nm. According to this figure, after the annealing process, the grain size of the as-grown film increases from 18 nm to 32 nm. It is seen from these figures that both the as-grown and annealed film surfaces are homogeneous and crack-free. The film thickness was also determined as 688 nm from the cross-sectional SEM micrograph of deposited indium sulfide thin film.

### 3.2. Optical properties of indium sulfide thin films

The absorbance ($A$) and transmittance ($T$) spectra of the InS thin films are shown in Figures 3a and 3b, respectively. The optical properties of the films were determined from the transmission measurements in the wavelength range of 300–1100 nm. As can be seen from this figure, the optical transmittance of the deposited films was in the range of 52%–22% at a wavelength of 550 nm, while it decreases to a value of 26% after heat

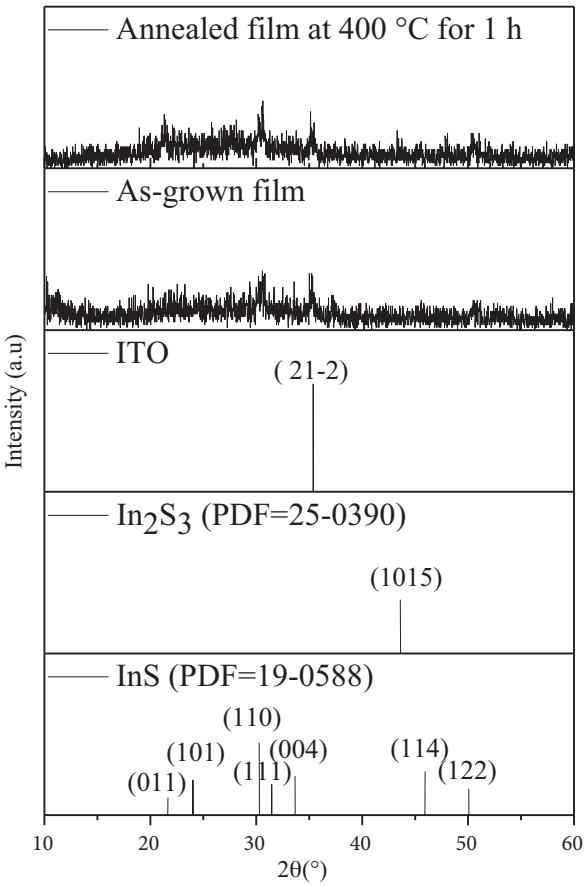


**Figure 1.** X-ray diffraction pattern of as-grown and annealed InS thin film deposited at 60 h with the thickness of 688 nm.

treatment. The optical energy band gaps of both as-grown and annealed films were determined from the optical absorption spectra by using the following expression:

$$\alpha h\nu = B(h\nu - E_g)^n, \tag{1}$$

where $B$ is a constant, $h$ is Planck's constant, $\nu$ is the frequency of the incident photon, and the exponent $n$ depends on the type of electronic transition. $n$ may have values of 1/2 and 2 corresponding to the allowed direct and allowed indirect transitions, respectively. In Eq. 1, $\alpha$ is the linear absorption coefficient given by:

$$\alpha = \frac{2.303A}{d}, \tag{2}$$

where $A$ is the absorbance and $d$is the film thickness. The direct and indirect band gap values ($E_g$) were determined by extrapolating the linear part of the plots $(\alpha h\nu)^2$ vs. $h\nu$ and $(\alpha h\nu)^{1/2}$ vs. $h\nu$ in the abscissa (x axis), which indicate the allowed direct and allowed indirect transitions in the deposited films, respectively. $(\alpha h\nu)^2$ vs. $h\nu$ and $(\alpha h\nu)^{1/2}$ vs. $h\nu$ plots are shown in Figure 4 for as-grown and annealed InS thin films. The calculated direct band gap energy of the InS films decreased from 2.31 eV to 2.19 eV with increasing film thickness and grain size. Moreover, the indirect band gap of the films decreased from 1.89 eV to 1.75 eV, except for the thin film having thickness of 688 nm listed in the Table. These values are in agreement with

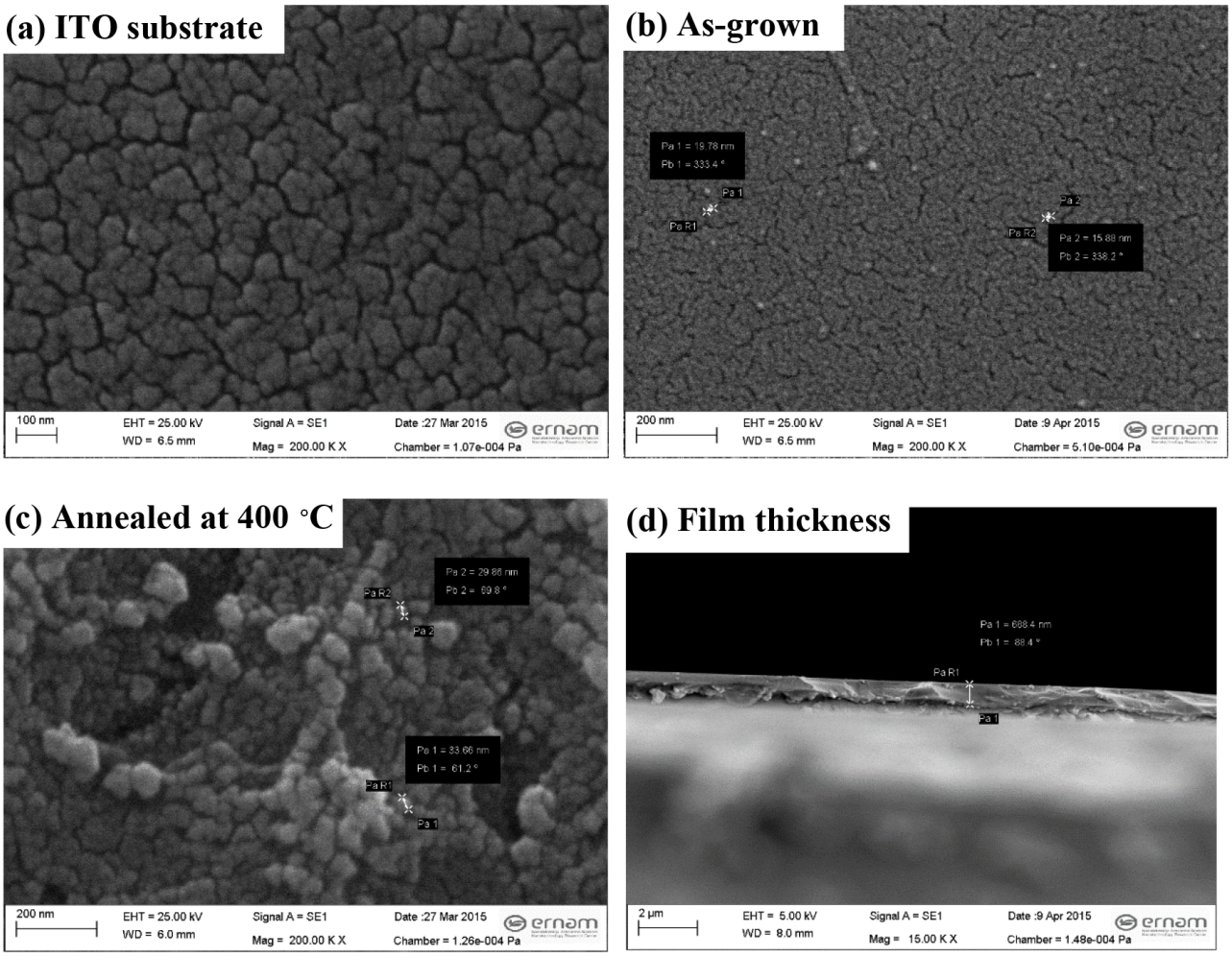


**Figure 2.** SEM images of (a) ITO substrate, (b) as-grown indium sulfide thin film deposited at 60 h with the thickness of 688 nm, (c) annealed at 400 °C, and (d) film thickness.

the literature [3,7]. Decrement both in direct and indirect band gap ($E_g$) values of the films is due to the increasing grain size. Some authors have reported that the $E_g$ shortening is attributed to increasing defects (e.g., displacements of atoms and lattice disorders) in the films, which produce localized states in the band structure and are responsible for the low value of $E_g$ [9]. This behavior is also supported by the SEM pictures in Figure 2. A reduction in band gap energy from 2.31 eV to 2.19 eV results in increasing grain size from 18 nm to 32 nm with annealing. The band gap energy values of as-grown and annealed films are listed in the Table.

The refraction index ($n$) and extinction coefficient ($k$) of indium sulfide thin films are given by the following formulas [10]:

$$k = \frac{\alpha\lambda}{4\pi}, \tag{3}$$

$$n = \frac{1+R}{1-R} + \sqrt{\frac{4R}{(1-R)^2} - k^2}. \tag{4}$$

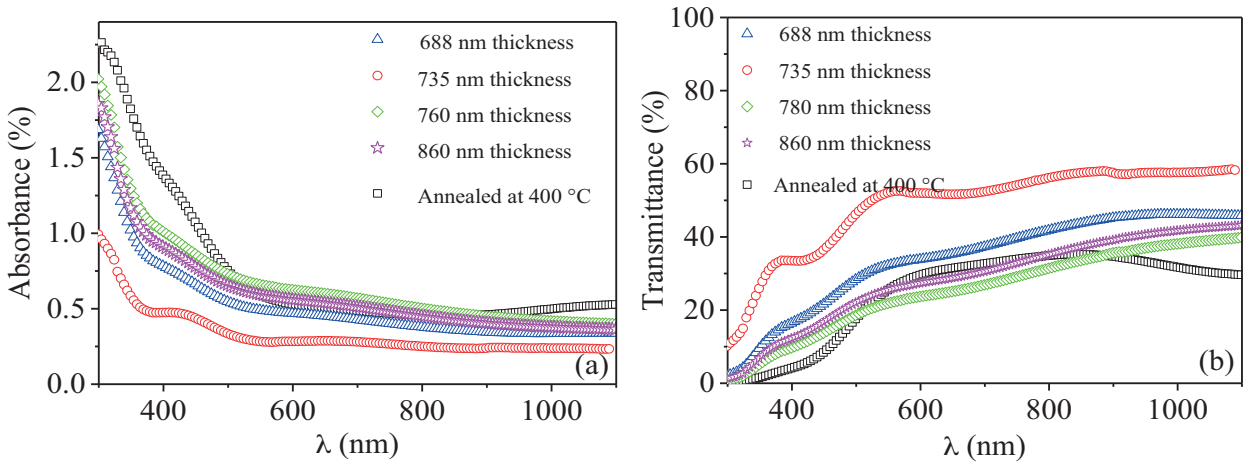


**Figure 3.** Optical (a) absorbance and (b) transmittance spectra of as-grown indium sulfide thin films with different thicknesses and annealed film deposited at 60 h with the thickness of 688 nm.

**Table.** Film thickness, grain size, optical parameters, and sheet resistivity of as-grown and annealed indium sulfide thin films at $\lambda\lambda = 600$ nm.

| Thickness (nm) | Grain size (nm) | Direct $E_g$ (eV) | Indirect $E_g$ (eV) | $n$ | $k$ | $\varepsilon_1$ | $\varepsilon_2$ | $\rho(\Omega$ cm) |
|---|---|---|---|---|---|---|---|---|
| 688 (as-grown) | ~ 18 | 2.31 | 1.61 | 2.69 | 0.32 | 7.14 | 1.73 | 33 |
| 735 (as-grown) | ~ 20 | 2.26 | 1.89 | 2.21 | 0.18 | 4.84 | 0.80 | 32 |
| 780 (as-grown) | ~ 23 | 2.23 | 1.80 | 3.10 | 0.38 | 9.46 | 2.34 | 31 |
| 860 (as-grown) | ~ 27 | 2.22 | 1.78 | 2.95 | 0.31 | 8.59 | 1.81 | 29 |
| 688 (annealed) | ~ 32 | 2.19 | 1.75 | 2.84 | 0.36 | 7.92 | 2.06 | 28 |

The refractive index and extinction coefficient of indium sulfide thin films are shown in Figures 5a and 5b, respectively. It was determined from these figures that both the refractive index and extinction coefficient values varied in the range of 2.21–3.10 and 0.18–0.38, respectively, for the as-grown and annealed InS thin films at a 600 nm wavelength, as tabulated in the Table. Our $n$ and $k$ values are in good agreement with the reported data ($n \approx 2.50$ and $k \approx 0.2$ at a wavelength of 600 nm) for InS prepared by the thermal evaporation method [11].

The real ($\varepsilon_1$) and imaginary ($\varepsilon_2$) parts of the dielectric constants are expressed as follows:

$$\varepsilon_1 = n^2 - k^2, \tag{5}$$

$$\varepsilon_2 = 2nk. \tag{6}$$

Figures 6a and 6b show the dependence of $\varepsilon_1$ and $\varepsilon_2$ on wavelength, respectively. It was clearly seen that both $\varepsilon_1$ and $\varepsilon_2$ change in the range of 4.84–9.46 and 0.80–2.34, respectively, for the as-grown and annealed InS thin films at a wavelength of 600 nm as seen in the Table. It should be noted that the $\varepsilon_2$ values in our calculations were found to be higher than the value ($\varepsilon_2 \approx 0.6$ at $\lambda = 600$ nm) given by Seyam [11].

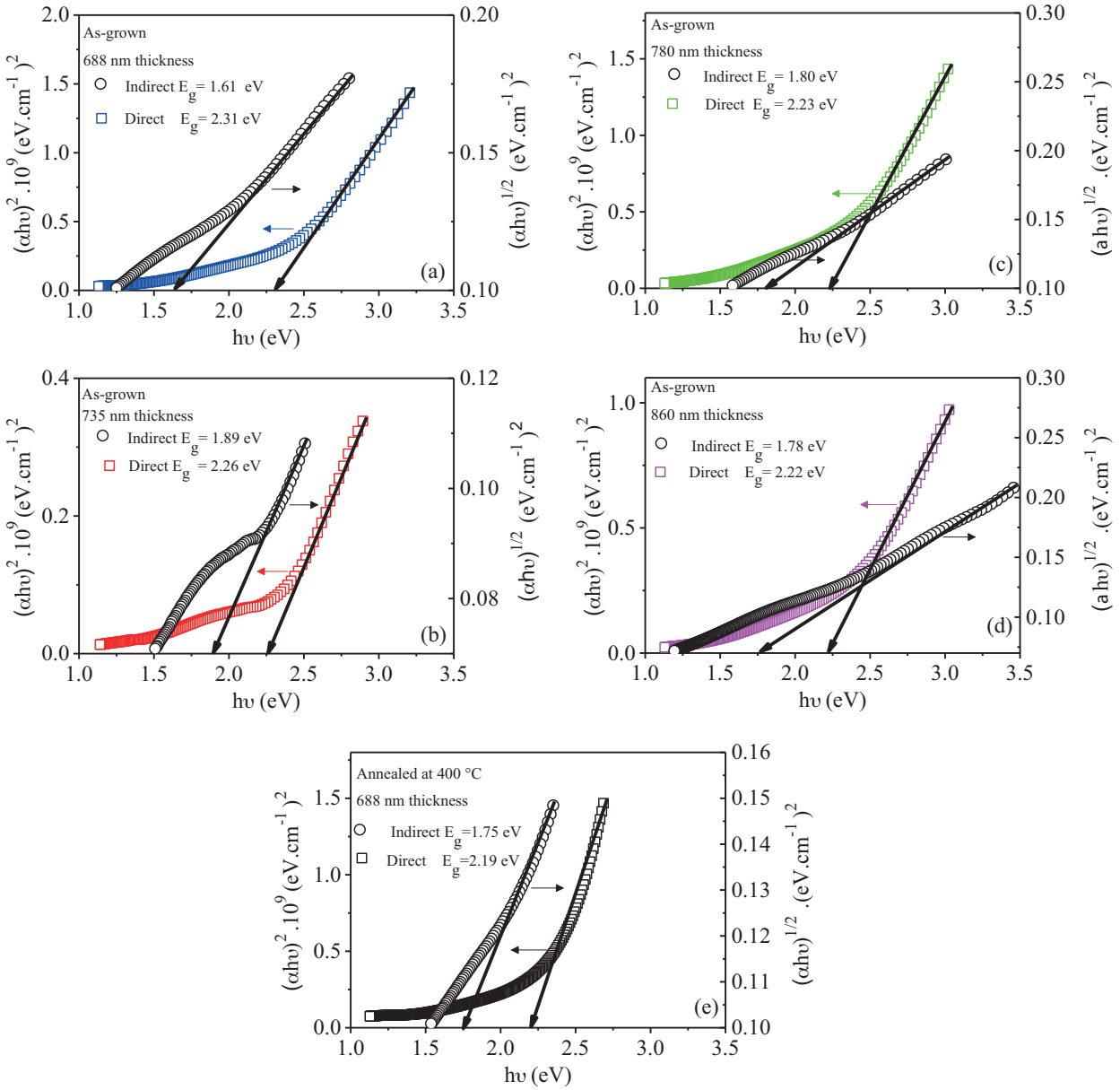


**Figure 4.** The dependence of $(\alpha h\nu)^2$ vs. $h\nu$ and $(\alpha h\nu)^{1/2}$ vs. $h\nu$ for as-grown and annealed InS thin films with different thicknesses of (a) 688 nm, (b) 735 nm, (c) 780 nm, and (d) 860 nm and (e) annealed film as-grown at 60 h with the thickness of 688 nm.

### 3.3. Electrical properties of indium sulfide thin films

The sheet resistivity ($\rho$) of the ITO substrate without coated film was measured as 34 Ω cm. The $\rho$ value of the as-grown and annealed films decreased from 33 Ω cm to 28 Ω cm, as shown in the Table. A reduction in $\rho$ may be due to the increasing film thickness and grain size from ∼18 nm to ∼32 nm as confirmed by the SEM pictures (Figure 2) and listed in the Table. Grain boundary scattering of free electrons in thicker films is less than in thinner films because of larger crystallite sizes. Since $\rho$ is proportional to the electron scattering frequency, $\gamma(1/\rho = N_e e^2/m_e^*\gamma)$, $\rho$ decreases with increasing film thickness [12–14]. Moreover, a decrement in

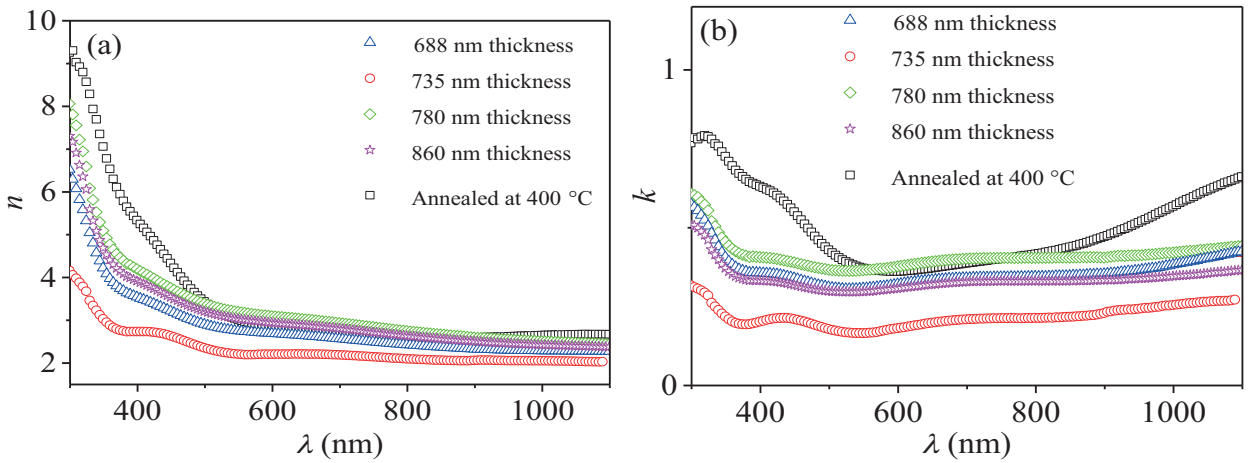


**Figure 5.** The variation of (a) refractive index and (b) extinction coefficient of as-grown indium sulfide thin films with different thicknesses and annealed film deposited at 60 h with the thickness of 688 nm.

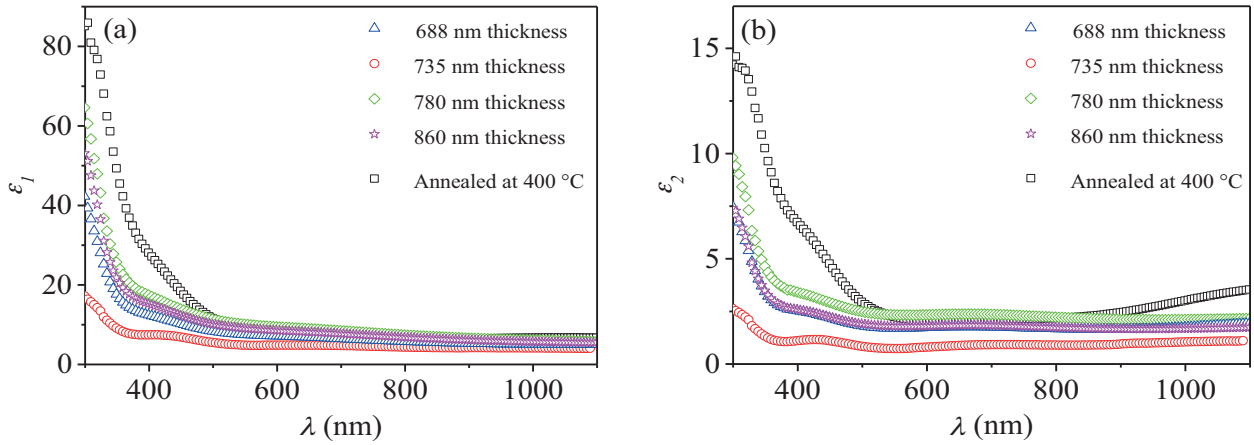


**Figure 6.** The variation of (a) real and (b) imaginary parts of as-grown indium sulfide thin films with different thicknesses and annealed film deposited at 60 h with the thickness of 688 nm.

$\rho$ could be attributed to an increment in electron density or mobility [$n = 1/q\rho\mu_n$ (where $n$ is the electron density, $q$ is the electronic charge, and $\mu_n$ is the electron mobility)] [14,15].

## 4. Conclusion

In this work, we report the effect of deposition time (60 h, 63 h, 66 h, and 69 h) and thermal annealing (400 °C) on the structural, optical, and electrical properties of InS thin films deposited onto ITO substrates at room temperature by CBD. The obtained films were polycrystalline with an orthorhombic crystal structure. The grain size of the InS thin films increased from 18 nm to 32 nm with annealing. At a wavelength of 550 nm, the optical transmission of the deposited InS films varied between 52% and 22%. It fell to 26% after the annealing process. With increasing film thickness and grain size, the direct and indirect optical band gap values of the films decreased from 2.31 eV to 2.19 eV and from 1.89 eV to 1.75 eV, respectively. The refractive index, extinction coefficient, and real and imaginary parts of the dielectric constant of all the films were also calculated. Moreover, the sheet resistivity of the films decreased slightly from 33 Ω cm to 28 Ω cm with increasing grain

size. In conclusion, we think that annealed film with the highest grain size, lower resistivity, and suitable optical properties may be promising material for solar cell applications.

**Acknowledgment**

This work was financially supported by the Mehmet Akif Ersoy University Scientific Research Projects Coordination Unit under project number 0201-NAP-13.

## References

[1] Rodriguez, M.; Silver, A.; Ortiz, A.; Sanchez; A. *Thin Solid Films* **2005**, *480-481*, 133-137.

[2] Trigo, J. F.; Asenjo, B.; Herrero, J.; Gutierrez, M. *Sol. Energy Mater. Sol. Cells* **2008**, *92*, 1145-1148.

[3] Ranjitha, R.; Johna, T.; Karthaa, C., Vijayakumara, K.; Abeb, T.; Kashiwabab, Y. *Mater. Sci. Semiconductor Processing* **2007**, *10*, 49-55.

[4] Bayon, R.; Guillen, C.; Martinez, M. A.; Gutierrez, M. T.; Herrero, J. *Electrochem. Soc.* **1998**, *145*, 2775.

[5] Timoumi, A.; Bouzouita, H.; Kanzari, M.; Rezig, B. *Thin Solid Films* **2005**, *480-481*, 124-128.

[6] Stoll, S.; Barron, R. *Chem. Mater.* **1998**, *10*, 650-657.

[7] Otto, K.; Katerski, A.; Mere, A.; Volobujeva, O.; Krunks, M. *Thin Solid Films* **2011**, *519*, 3055-3060.

[8] Lokhande, C. D.; Ennaoui, A.; Patil, P. S.; Giersig, M.; Diesner, K.; Muller, M.; Tributsch, H. *Thin Solid Films* **1999**, *340*, 18-23.

[9] Robles, R.; Vega, A.; Mokrani, A. *Opt. Mater.* **2001**, *17*, 497-499.

[10] Benramdane, N.; Murad, A.; Misho, H.; Ziane, M.; Kebbab, *Z*. *Mater. Chem. Phys.* **1997**, *48*, 119.

[11] Seyam, M. A. M. *Vacuum* **2001**, *63*, 441-447.

[12] Lugo-Loredo, S.; Peña-Méndez, Y.; Calixto-Rodriguez, M.; Messina-Fernández, S.; Alvarez-Gallegos, A.; Vázquez-Dimas, A.; Hernández-García, T. *Thin Solid Films* **2014**, *550*, 110-113.

[13] Göde, F.; Güneri, E.; Emen, F. M.; Kafadar, V.; Ünlü, S. *J. Lum.* **2014**, *147*, 41-48.

[14] Zhao, Z.; Morel, D. L.; Ferekides, C. S. *Thin Solid Films* **2002**, *413*, 203-211.

[15] Sze, S. M. *Physics of Semiconductor Devices*, 2nd ed.; Wiley: New York, NY, USA, 1981.